iJRASET
International Journal For Research in Applied Science and Engineering Technology

INTERNATIONAL JOURNAL FOR RESEARCH

IN APPLIED SCIENCE & ENGINEERING TECHNOLOGY

Volume: 6 **Issue:** XII **Month of publication:** December 2018

DOI: http://doi.org/10.22214/ijraset.2018.19536

www.ijraset.com

Call: 08813907089 | E-mail ID: ijraset@gmail.com

International Journal for Research in Applied Science & Engineering Technology (IJRASET)
ISSN: 2321-9653; IC Value: 45.98; SJ Impact Factor: 6.887
Volume 6 Issue XII, Dec 2018- Available at www.ijraset.com

Quantum Chemical and Adsorptive Studies of Euphorbia Hirta as Corrosion Inhibitor of Mild Steel in Hydrochloric Acid

Komal Choudhary[1], Arpita Sharma[2], Monika[3], Anju4, Alka Sharma[5]
[1, 2, 3, 4, 5]*Centre of Advanced Study, Department of Chemistry, University of Rajasthan, Jaipur-302 004 (Rajasthan) India*

Abstract: ***Inhibitory propensity of ethanolic extract of Euphorbia hirta (EEEh) was investigated for mild steel (MS) in 0.5 M HCl at room temperature (30°C). Chemical method was employed to study the effect of change in concentration and immersion periods on inhibitory efficacy of EEEh. Corrosion, kinetic and adsorptive parameters were evaluated and various characterization techniques, viz., UV-Visible spectroscopy, FT-IR spectroscopy, QCA, SEM, EDX, AFM, optical micrographs were employed to elucidate the adsorptive propensity of its phytochemicals on MS surface. The percentage inhibitory efficacy (IE%) of EEEh was observed maximum (84.07%) at its 1.02 gm/L concentration. EEEh follows Langmuir adsorption isotherm with physisorption mode of adsorption. QCA reveal that the constituents of EEEh have active adsorption centres consequently forming a protective film over MS surface which is evident by OM, SEM-EDX and AFM.***
Keywords: Acid corrosion, Euphorbia hirta, adsorption, QCA, SEM-EDX, AFM.

I. INTRODUCTION

The study of the corrosion behaviour of various metals in corrosive media has continued to attract considerable attention because of the many important applications of the metals [1]. The corrosion inhibition of mild steel (MS) is of such interest because of its varied significant industrial usages. Acids, particularly hydrochloric acid are widely used for the pickling, cleaning, descaling, and so on of iron and steel [2]. Corrosion inhibitors are generally used in these processes to control the dissolution of the metal and well-known acid corrosion inhibitors are organic, inorganic compounds containing O-, N-, and chromium atoms [3–4]. But due to the environmental legislations [5–6], now-a-days, much interest has grown to use biocompatible and biodegradable natural resources as ecofriendly and nonStoxic *green* inhibitors [7–15].

Literature survey revealed that weed E. hirta contains mainly alkaloids, triterpenoids, flavonoid, tannins, steroids, glycosides, phenolic acids, gallic acids, protocatechuic acids, ß-amyrin, ajzerin, rutin, Quercitin etc. and each of these compounds have adsorptive propensity [16–17].

Structures of some of the major phytochemicals present in *Euphorbia hirta* are as follows:

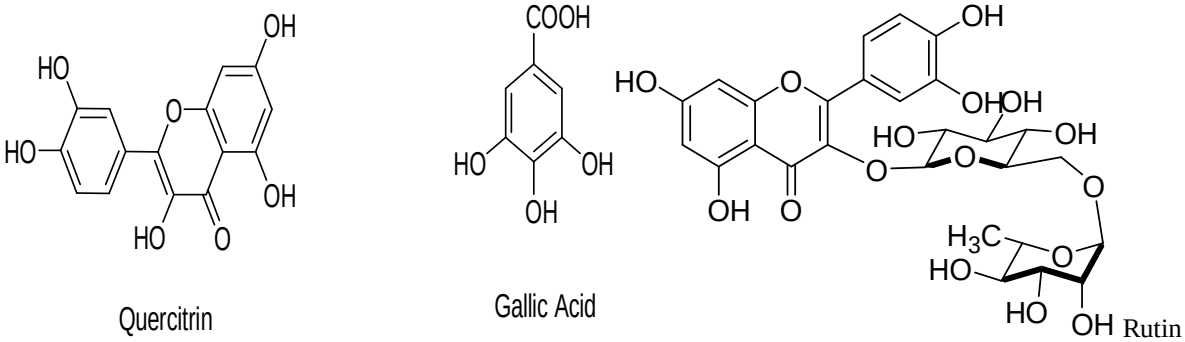

II. EXPERIMENTATION

A. *Specimen Preparation*

Composition of metal coupons {Fe 99.7%, (Mn) 0.3%, (Mo) 0.01%, (Cr) 0.039%} was determined by X-Ray fluorescence analysis. MS sheet was cut in to rectangular coupons having dimensions ($3\times2.4\times0.16 cm^3$) with a small hole of 0.12 mm diameter near upper edge for hanging in test media. Prior to all measurements, surface treatment was given to each coupon and were placed in the desiccators [7–11], [13], [18–19].

ISSN: 2321-9653; IC Value: 45.98; SJ Impact Factor: 6.887
Volume 6 Issue XII, Dec 2018- Available at www.ijraset.com

*B. Preparations of Electrolyte and Ethanolic Extract of E. Hirta (*EE*Eh)*

Triple distilled water and AR grade HCl were used for preparation of 0.5 MHCl [18–19]. The stock solution of ethanolic extract of *E. hirta* was prepared as per standard procedures [7–11], [13], [18–19]. The mass of EE*Eh* compounds was accessed to be 0.33g/mL. The presence of alkaloids and triterpenoids and other constituents was verified by thin layer chromatography (TLC) technique. Chromatography was performed in the following solvent systems: Nonpolar solvent: toluene-acetone (8:2); semi-polar solvent: toluene-chloroform-acetone (40:25:35); polar solvent: n-butanol-glacial acetic acid-water (50:10:40). The chromatograms were observed first without chemical treatment, under UV 254 nm and UV 365 nm light, and then using the spray staining reagent giving an orange and blue spot on preparative silica gel TLC [17].

C. Preparation of test solutions

Seven separate beakers were labelled as MS0, MS1, MS2, MS3, MS4, MS5, and MS6, each containing 100 ml of electrolyte (0.5 M HCl) solution. EE*Eh* was added in order of increasing concentration as to have 0.032, 0.12, 0.24, 0.42, 0.60, and 1.02 g/L respectively in MS1, MS2, MS3, MS4, MS5, MS6 etc. No extract was added to MS0, i.e., the first beaker solution. All the beakers were covered with Teflon tape and kept unstirred throughout the experiment.

D. Chemical measurements

Chemical method is probably the most widely used method to determine the effectiveness of EE*Eh* as corrosion inhibitor. Surface treated MS coupons were weighed using an analytical balance (Adair Dutt 205 ACS) before and after immersion in 100 ml of the test solution for the studied immersion periods. Average mass loss for each of the identical experiments was taken and expressed in gm and various corrosion parameters were evaluated [7–11], [13], [18–19].

E. Quantum Chemical calculations and analysis

Quantum chemical analyses were carried out by using the PM3 method of the quantum chemical Package MOPAC 6.0 of Hyperchem 7.5 software. The energy of the highest occupied molecular orbital (E_{HOMO}) and the lowest unoccupied molecular orbital (E_{LUMO}), energy band gap, $\Delta E = E_{HOMO}-E_{LUMO}$, value of binding energy, heat of formation and the dipole moment (μ) were used to elucidate the adsorptive centres of the phytochemicals of *E. hirta* [20-22].

F. Spectrophotometric Analysis

1) *UV-Visible Spectroscopy*: To confirm the possibility of the formation of EE*Eh*-Fe complex, conventional and most sensitive direct spectrophotometric technique based on UV–Visible absorption was used with the help of quartz glass cell in 400-800 nm visible range. Spectras were recorded for MS coupons immersed in test solutions without (blank) and with varied concentrations of EE*Eh* [23].
2) *Fourier-Transform Infrared (FT-IR) Spectroscopy*: FT-IR spectrum of EE*Eh* and surface-adsorbed protective film was recorded by employing KBr pellets method in the range 4000 to 400 cm^{-1} (8400 Shimadzu, Japan) [7–11], [13], [18–19].

G. Surface Morphological Studies

Optical micrography (OM), Scanning Electron Microscopy (SEM) and Energy dispersive X-ray analysis (EDX)

Surface morphology of coupons was analysed using Optical microscope (LABOMED) on 25μ and Scanning Electron Microscope (ZEISS).

1) *Atomic Force Microscopy (AFM):* Atomic force microscopy (Nanonics MultiView 2000 TM model) was used with the image scanning area as 5μm×5μm and the scan rate 0.5 HZ/s to characterize coupons' surface and various parameters (height, amplitude, error and phase signals) endorsed the formation of a protective film over the coupon surface immersed with *EE*Eh.

III. RESULTS AND DISCUSSION

The experimental data were used to evaluate various corrosion and adsorptive parameters such as weight loss (mg), corrosion rate (ρ_{corr}) (mmy^{-1}), percentage inhibition efficiency (IE %), fractional surface coverage (θ), adsorption equilibrium constant (K_{ad}) which have been tabulated in the Table 1. Plot of weight loss against immersion time for MS in 0.5 MHCl without (blank) and with varied concentrations of EE*Eh* at 30ºC (Fig.1) shows maximum weight loss (40.20×10^{-2} mg) at maximum (72h) immersion. Addition of additives (1.02 g/L) reduces loss in weight (6.4×10^{-2} mg) significantly, clearly depicts the inhibitory propensity of EE*Eh*.

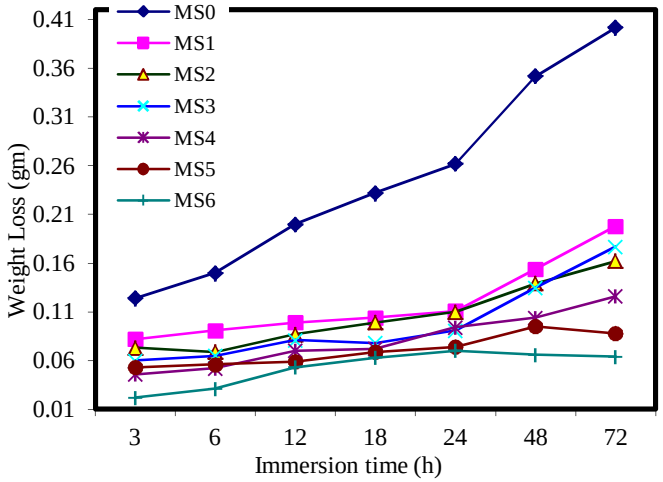

Fig.1 Loss in weight Vs. immersion period for MS corrosion in 0.5 M HCl without and with different concentrations of EE*Eh* at 30°C.

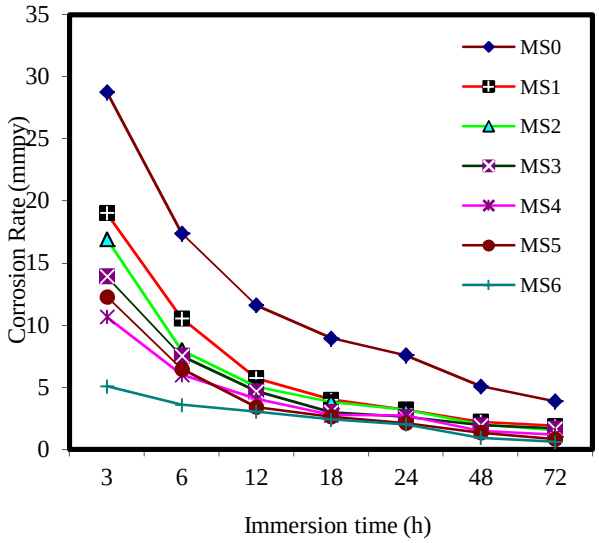

Fig.2 Corrosion rate Vs. Immersion period (h) without and with various without and with concentrations of EE*Eh* on acid corrosion of MS at room temperature (30°C).

Results in Table 1clearly exhibit the inhibitory efficacy of EE*Eh* for MS in 0.5 M HCl. It is evident from Table 1 and Fig. 2 that the maximum corrosion rate has been observed to be 28.78×10^{-3} (mmy^{-1}) at 3 h in without inhibitor condition and the minimum corrosion rate were observed 0.61×10^{-3} (mmy^{-1}) at 72 h immersion period at highest concentration of 1.02 g/L of EE*Eh*.

A. Corrosion and adsorptive parameters

It is clear from Table 1 and Fig. 3 that the inhibition efficiency (IE %) of EE*Eh* is maximum (84.07 %) at its 1.02 g/L concentration. This can be attributed to the adsorption of phytochemicals of EE*Eh* on MS surface thereby minimizing MS dissolution by blocking its corrosion sites and hence decreasing the corrosion rate. The presence of phenolic and flavonoid aromatic rings with several π-electrons systems containing O- atoms in phytochemicals of EE*Eh* and the presence of vacant d-orbitals in iron can induce the greater surface coverage of the inhibitor molecule onto the MS surface. It has been reported by a number of authors that the formation of donor-acceptor surface complexes between free electrons of an inhibitor and a vacant d-orbital of a metal is responsible for the inhibition of the corrosion process [24].

TABLE 1

Various Corrosion parameters of acid corrosion of mild steel without and with various concentration of EEEh at various immersion periods (h) at room temperature (oC)

Immersion period (h)	EEEh Conc. (g/L)	Corrosion parameters					
		Weight loss (mg)×10^{-2}	Corrosion rate (ρ_{Corr})×10^{-3}	Inhibition efficiency (IE%)	Functional surface coverage (Θ)	Adsorption Equilibrium Constant (K_{ad})	Gibbs free energy (ΔG)
3	MS-0	12.4	28.78	-	-	-	-
	MS-1	8.2	19.03	33.87	0.3387	17.07	-17.26
	MS-2	7.3	16.94	41.12	0.4112	5.82	-14.55
	MS-3	0.06	13.92	51.61	0.5161	4.44	-13.87
	MS-4	4.6	10.67	62.90	0.6290	4.03	-13.63
	MS-5	5.3	12.30	57.25	0.5725	2.23	-12.14
	MS-6	2.2	5.10	82.25	0.8225	4.54	-13.93
6	MS-0	1.5	17.40	-	-		
	MS-1	9.1	10.56	39.33	0.3933	21.61	-17.86
	MS-2	6.7	8.08	54	0.54	9.78	-15.86
	MS-3	6.5	7.54	56.66	0.5666	5.44	-14.38
	MS-4	5.2	6.03	65.33	0.6533	4.48	-13.39
	MS-5	5.6	6.49	62.66	0.6266	2.79	-12.71
	MS-6	1.9	3.59	79.33	0.7933	3.76	-13.45
12	MS-0	15.0	11.60	-	-		
	MS-1	9.1	5.74	50.5	0.5050	34.00	-19.00
	MS-2	6.9	5.04	56.5	0.5650	10.82	-16.11
	MS-3	6.5	4.70	59.5	0.5950	6.12	-14.68
	MS-4	5.2	4.06	65	0.6500	4.42	-13.86
	MS-5	5.6	3.42	70.5	0.7050	3.98	-13.60
	MS-6	3.1	3.07	73.5	0.7350	2.71	-12.63
18	MS-0	23.2	8.97	-	-		
	MS-1	10.4	4.02	55.17	0.5517	41.02	-19.47
	MS-2	9.9	3.82	57.32	0.5732	11.19	-16.20
	MS-3	7.8	3.01	66.37	0.6637	8.22	-15.42
	MS-4	7.2	2.78	68.96	0.6896	5.29	-14.31
	MS-5	6.9	2.66	70.25	0.7025	3.93	-13.57
	MS-6	6.3	2.43	72.84	0.7284	2.62	-12.55
24	MS-0	26.2	7.60	-	-		
	MS-1	11.1	3.22	57.63	0.5763	45.34	-19.72
	MS-2	11.0	3.19	58.01	0.5801	11.51	-16.27
	MS-3	9.1	2.64	65.26	0.6526	7.82	-15.30
	MS-4	9.4	2.72	64.122	0.6412	4.25	-13.76
	MS-5	7.4	2.14	71.75	0.7175	4.23	-13.75
	MS-6	7.0	2.03	73.28	0.7328	2.68	-12.61
48	MS-0	35.2	5.10	-	-		
	MS-1	15.4	2.23	56.25	0.5625	42.85	-19.58
	MS-2	13.9	2.01	60.51	0.6051	12.76	-16.53
	MS-3	13.5	1.95	61.64	0.6164	6.69	-14.90
	MS-4	10.4	1.50	70.45	0.7045	5.67	-14.49
	MS-5	9.5	1.37	73.01	0.7301	4.50	-13.91
	MS-6	6.6	0.95	81.25	0.8125	4.24	-13.76
72	MS-0	40.2	3.88	-	-		
	MS-1	19.8	1.91	50.74	0.5074	34.34	19.02
	MS-2	16.2	1.56	59.70	0.5970	12.34	16.45
	MS-3	17.7	1.71	55.97	0.5597	5.29	14.31
	MS-4	12.6	1.21	68.65	0.6865	5.21	14.27
	MS-5	8.8	0.85	78.10	0.7810	5.94	14.61
	MS-6	6.4	0.61	84.07	0.8407	5.17	14.26

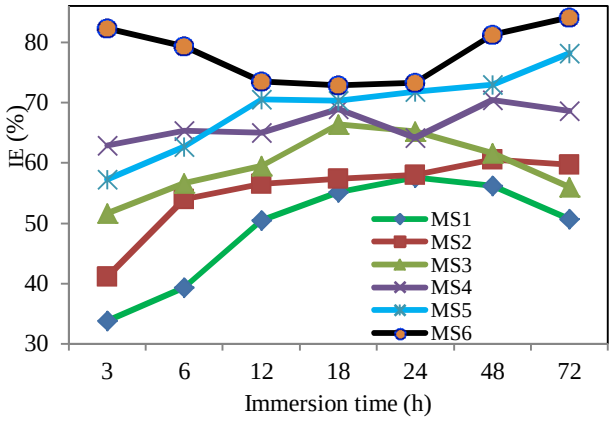

Fig. 3 Inhibition efficiency (IE %) Vs. Immersion period (h) with various concentration of EE*Eh* on acid corrosion of MS at room temperature (30°C).

B. Adsorption Isotherm (Mechanism of Inhibition)

Adsorption isotherm provides useful insights into the mechanism of corrosion inhibition. The action of inhibitor in acid solutions is generally agreed to be adsorption on to the metal surface which is usually oxide free in acid solutions. The adsorption of an inhibitor species in and on the metal surface-solution interface can be expressed as a place exchanger process between the inhibitor molecules in the acidic solutions and the water molecule on the metallic surface.

$$Inh._{aq} + x\,H_2O_{ads} \leftrightarrow Inh._{ads.} + x\,H_2O_{aqs}$$

Here x is the size ratio, representing the number of water molecules displaced by one molecule of inhibitor during adsorption process. Attempts were made to fit the surface coverage (θ) values to various adsorption isotherm, including Langmuir, Frumkin, Freunlich and Temkin El-Awady. By far the best results were obtained fitting Langmuir adsorption isotherm. The relation between the surface coverage (θ) defined by (I.E% /100) and the concentration (C) can be represented by the Langmuir isotherm that is K_{ad}, is expressed as: $(C/\theta) = C + 1/K_{ad}$ or $K_{ad}C=\theta/(1-\theta)$

where C is the concentration of EE*Eh* in g/L; θ the fractional surface coverage and K represents the equilibrium constant for the adsorption/desorption process of the inhibitor molecules on to the metal surface The fractional surface coverage (θ) and the adsorption equilibrium constant (K_{ad}) have been found large at higher concentration of EE*Eh*, hence the higher concentration of EE*Eh* is essential for maximum adsorption over MS surface. The best fitted straight line was obtained for the plot of C_{inh}/θ versus C_{inh} with slopes around unity and from the intercepts of the straight line C_{inh}/θ-axis, K value has been calculated [25–26].

TABLE 2

Correlation coefficient and slopes from langmuir adsorption isotherm at 72 h exposure periods at various concentrations and at room temperature.

Immersion time (h)	Correlation coefficient (R^2)	Slope	Adsorption coefficient (K) $\times 10^{-2}$
3	0.939	1.177	6.41
6	0.976	1.239	10.10
12	0.996	1.321	17.24
18	0.999	1.347	28.57
24	0.996	1.336	23.25
48	0.992	1.202	8.319
72	0.985	1.347	11.49

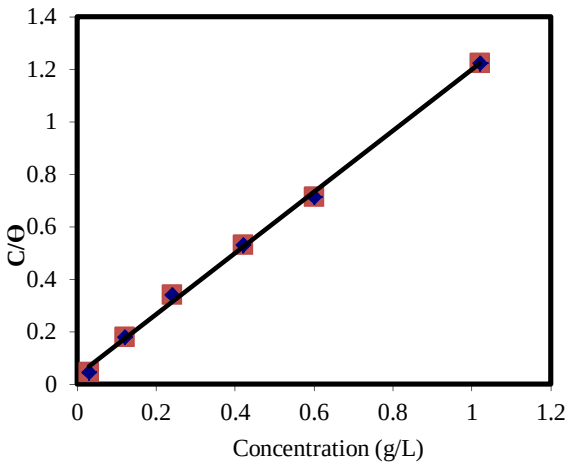

Fig. 4 Plot of C/θ Vs C in 72 h immersion period at optimum concentration 1.02 (g/L)

This isotherm postulates that there is no interaction between the adsorbed molecules, and the energy of adsorption is independent of the surface coverage. Langmuir isotherm assumes that the solid surface contains a fixed number of adsorption sites, and each holds one adsorbed species [26–27]. The equilibrium constant of adsorption K is related to the standard free energy of adsorption ΔG^{o}_{ads} kJ/mol., according to the expression: K = 1/ 55.5 exp [$-\Delta G^{o}_{ads}$/ RT], where 55.5 is the water concentration of solution. The free energy of adsorption, ΔG^{o}_{ads} was calculated and tabulated (Table 1) [27-28].

The negative values of ΔG^{o}_{ads} indicate that adsorbed layer on to the metal surface is stable and the adsorption process is spontaneous. It is well known that values of ΔG^{o}_{ads} of -20 kJ mol^{-1} or lower indicate a physical adsorption, while those of -40 kJ mol^{-1} or higher involve charge sharing or a transfer from the inhibitor molecules to the metal surface to form coordinate type of bond (chemisorption) [29–30]. The value of ΔG^{o}_{ads} was observed in the range from -19.78 to -12.02 kJ mol^{-1} thus suggesting the adsorption of EE*Eh* components involve physisorption type of interaction.

C. Quantum Chemical Analysis

Quantum chemical analysis (QCA) are employed to describe the adsorptive property and reactivity of the phytochemicals of inhibitors and their interactions with the metal surface [20], [32–34]. An attempt was made to evaluate the molecular orbital (FMO) density distributions of the inhibitor molecules present in ethanolic extract of *Euphorbia hirta* with the set of some independent variables like energy of HOMO, LUMO, dipole moment and Heat of Formation (Table 3). The optimized geometry of the compounds under investigation in their ground states was performed. Fig. 5 (a and e) shows the optimized molecular structure of Gallic acid and Quercitrin which are major chemical compounds [16–17]. It shows that the aromatic ring is in one plane, while the -OH and -COOH group is in another plane. According to the frontier molecular orbital theory, the formation of a transition state is due to an interaction between frontier orbitals of (HOMO and LUMO) of reacting species. HOMO is often associated with the capacity of a molecule to donate electrons, whereas LUMO represents the ability of the molecule to accept electrons. The electric/orbital density distributions of HOMO and LUMO for Gallic Acid and Quercitrin are shown in Table 3. Values of E_{HOMO} and E_{LUMO} are -9.319 and -0.614 eV and -8.526, -0.767 respectively. High values of E_{HOMO} are likely to indicate a tendency of the molecule to donate electrons to appropriate acceptor molecules with low-energy orbital. Higher values of the E_{HOMO} facilitate adsorption by influencing the electron transport process through the adsorbed layer. The lower the value of E_{LUMO}, the more probable, it is that the molecule would accept electrons. As for the values of ΔE (E_{LUMO}-E_{HOMO}) concern; lower values of the energy difference ΔE will cause higher inhibition efficiency because the energy to remove an electron from the last occupied orbital will be low. For the dipole moment (μ), higher values of μ will favour strong interaction of the inhibitor molecules with metal surface and lower values favour the accumulation of inhibitor molecules around electrode surface. The binding energy of EE*Eh* is found to be negative thus suggesting its constituents to be very stable and less prone to be split apart. The heat of formation of its molecules is negative which suggests that the formation is spontaneous and stable [32–34]. Quantum chemical parameters (Table 3) confirmed good inhibitory performance of active constituents of EE*Eh* and also confirmed strong interaction between these molecules and MS surface, thereby forming protective adsorptive layer at MS- inhibitor acid solution interface.

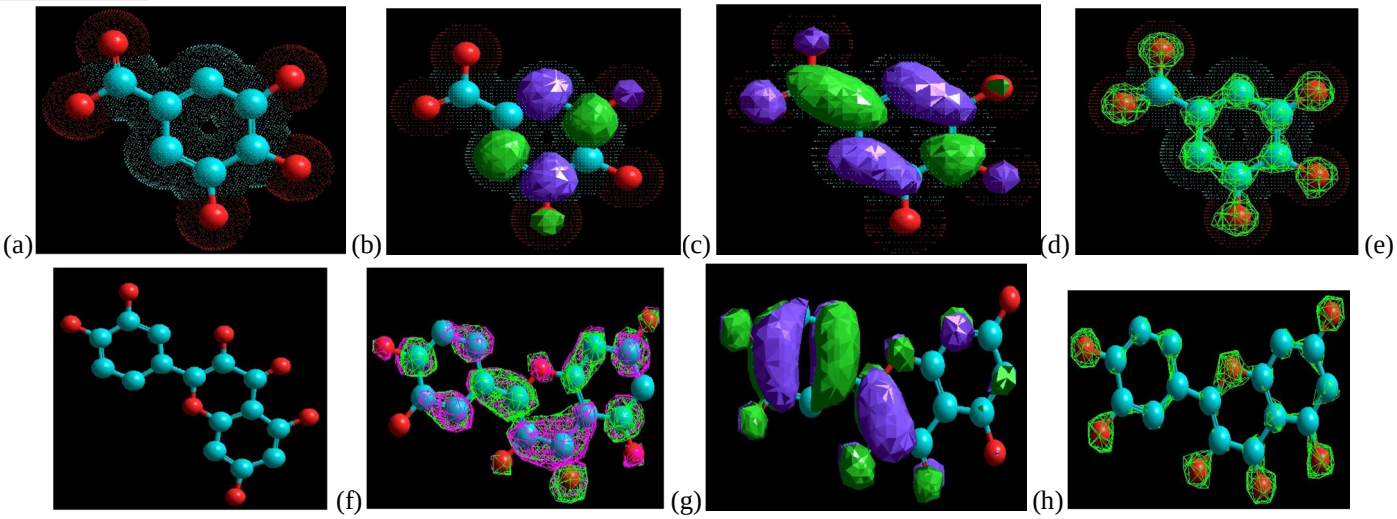

Fig.5 shows Optimized structures, LUMO structure, HOMO structure and 3-D- surface of Total Charge Density of Gallic acid (a-d) and Quercitrin (e-h).

TABLE 3
Calculated (energies & gradient) Quantum chemical parameters of Gallic acid & Quercitin of studied EEEh inhibitor

Name of the compound	Binding Energy (kcal/mol)	Heat of Formation (kcal/mol)	Dipole Moment (Debye)	E_{HOMO} (eV)	E_{LUMO} (eV)	$\Delta E = E_{HOMO} - E_{LUMO}$
Gallic acid	-2004.94	-33.89	1.872	-9.319	-0.614	-8.705
Quercitrin	-3718.71	-34.92	4.45	-8.526	-0.767	-7.759

D. Spectroscopic Analysis UV-Visible Spectroscopy

In order to confirm the possibility of the formation of EE*Eh* extract–Fe complex, UV-Visible absorption spectra were obtained for EE*Eh* and test solutions with MS immersed with 1.02 g/L EE*Eh* after 72 h. Figure 6: curve (a) is the spectrum of ethanolic extract of *Euphorbia hirta*, which gives the absorbance at 0.080 & λ_{max} is obtain in between 600-700 nm; curve (b) shows position of the absorbance with incubated MS at 0.025 &, & λ_{max} is obtain in between 600-700 nm. Fig.6 clearly indicate a deviation in absorbance values and their intensities. The change in the position of the absorbance maximum and wavelength maximum indicate the formation of a complex between two species in solution.

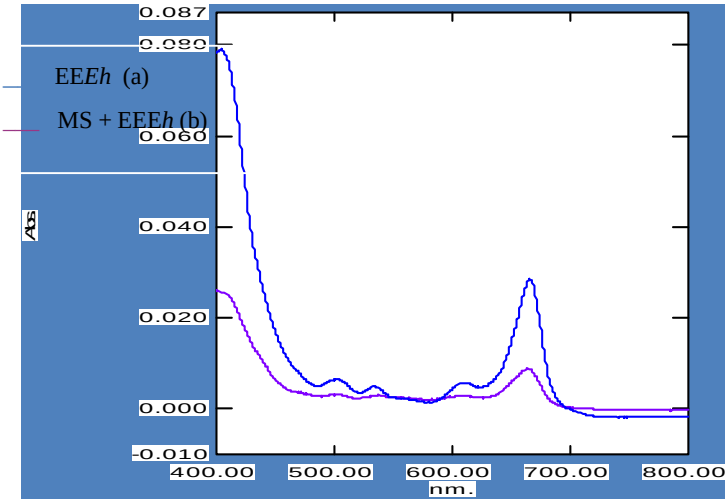

Fig.6 (a) & (b) UV-visible spectra of EE*Eh* and test solution with MS specimen immersed with EE*Eh* at 72h at room temperature.

However, there was no any significant change in the shape of the spectra but the absorbance decreases due to possible EE*Eh*-Fe complex, because absorbance are affected by change in concentration as well as chemical structure, thus confirm the possibility of the formation of EE*Eh*-Fe complex**.** Formation of this complex may be responsible for the observed deviation in the absorbance and its intensity value and this may be responsible for EE*Eh* anti-corrosion activity [35]. The organic compounds present in EE*Eh* get adsorbed on the metal surface thus impeding the corrosion of mild steel.

E. Fourier Transform- Infrared Spectroscopy Analysis

FT-IR spectroscopy is a powerful technique to determine the type of bonding for organic inhibitors adsorbed on the metal surface [35]. FT-IR spectra have been used to analyze the protective film formed on metal surface. FT-IR spectrum of EE*Eh* give the C=O stretching frequency around 1720 cm^{-1}, the broad spectrum of -O−H stretching frequencies around 3450 cm^{-1} and 3500 cm^{-1}, The bands ranging from 2950 to 3000 cm^{-1} can be attributed to –C–H stretching vibrations, the -C−O stretching frequency around 1100 cm^{-1}, and –OH stretching vibrations due to secondary alcohol around 1150-1200 cm^{-1} has decreased or diminished or even vanished from their pure peaks. This indicates that the functional groups are directly involved in metal-inhibitor interactions, resulting the formation of Fe^{2+} -EE*Eh* complex on the mild steel surface.

F. Surface Morphological Analyses Atomic Force Microscopy (AFM)

AFM is a powerful technique to investigative the surface morphology at nano-scale and has become a new choice to study the influence of inhibitor at the metal-solution interface [36–37]. AFM image analysis was performed to obtain the average roughness, Ra (the average deviation of all points roughness profile from a mean line over the evaluation length), root-mean-square roughness, Rq (the average of the measured height deviations taken within the evaluation length and measured from the mean line) and the maximum peak-to-height values. The three dimensional 3D-AFM morphologies and the AFM cross-sectional profile for polished mild-steel surface is shown in Fig.7 (a), mild steel surface immersed in 0.5 M HCl solutions (blank) is Fig.7 (b) and mild steel surface immersed in EE*Eh* at optimum concentrations is Fig.7 (c) respectively. It can be seen that the corrosion pattern of polished mild steel surface is appears uniform and the corrosion morphology of mild steel in blank 0.5 M HCl solution shown sharp mountain like shape, By contrast, the morphology of inhibited mild steel surface is looking smooth without any grooves. The mean roughness Rq and Ra and peak- to- peak values (Table 4) were calculated and these values indicate that in the presence of inhibitor the roughness of MS surface decreases due to the formation of the protective film onto the MS surface..

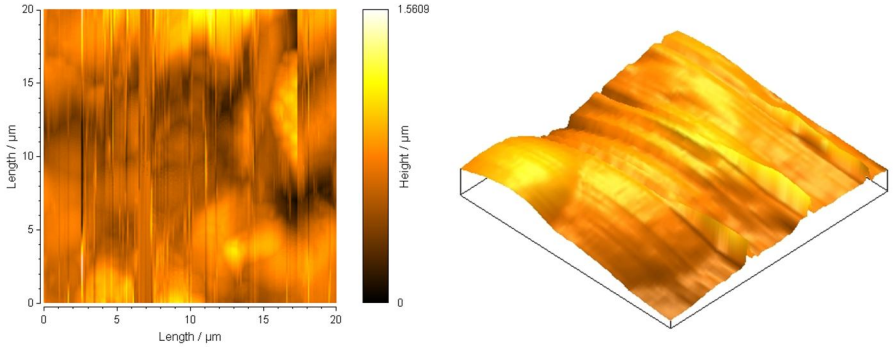

Fig.7 (a) Three dimensional (3D) AFM morphologies and the AFM cross-sectional profile for polished MS surface.

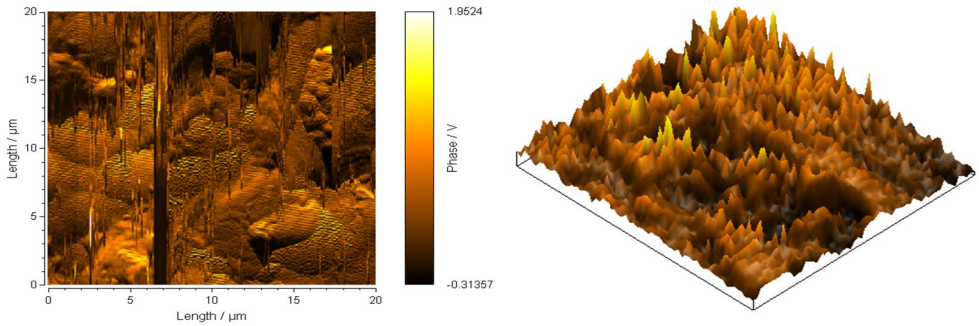

Fig.7 (b) AFM cross-sectional morphology and three dimensional (3D) morphologies of MS surface in blank (0.5 M) HCl.

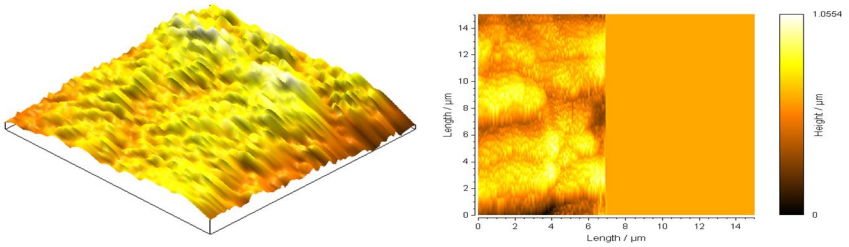

Fig.7 (c) AFM (3D) three dimensional morphologies and cross-sectional morphology of MS surface inhibited by 1.02 g/L EE*Eh* in 0.5 M HCl.

TABLE 4
Data of AFM for MS surface immersed in uninhibited and inhibited acidic environment.

Sample	RMS (Rq) Roughness (µm)	Average (Ra) Roughness (µm)	Mean (µm)	Peak-to-peak Height (µm)
MS Coupon	0.09	0.07	0.74	0.72
MS immersed in 0.5 M HCl	0.13	0.11	0.74	0.71
MS immersed in EE*Eh*+0.5 M HCl	0.09	0.11	0.68	0.83

G. Scanning Electron Microscopic and Optical Microscopic Examination

The SEM images of surface treated MS surface in 0.5 M HCl was seen uniformly smooth as illustrated in Fig.8 (a). Inspection of Fig. 8 (b) reveals that the MS surface after immersion in uninhibited 0.5 M HCl for 72 h shows an aggressive attack of the corroding medium on the MS surface. The corrosion products appear very uneven with black rough grooves. In contrast, in the presence of EE*Eh* inhibitor, Fig. 8 (c) shows that there is an adsorbed film on mild steel surface exposed to 0.5 M HCl solutions containing EE*Eh*, which do not exist in Fig. 8 (b). Thus, it can be concluded that the adsorbed film effectively inhibit the MS surface and impede its further dissolution in aggressive medium [38].

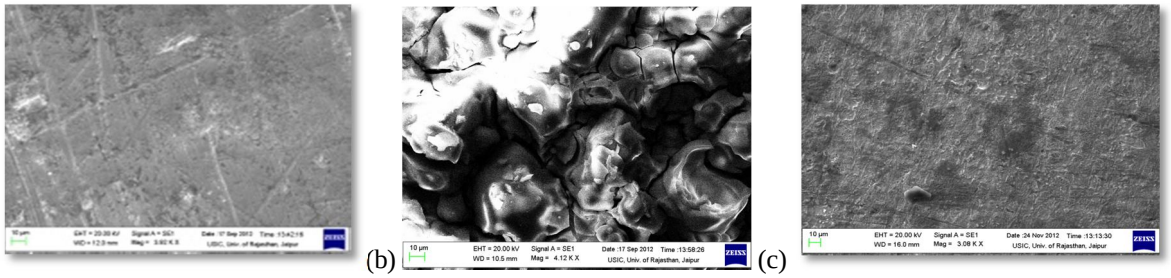

Fig.8 SEM micrographs of MS surface at 30ºC: (a) before immersion in aggressive medium; (b) after 72 h of immersion in 0.5 M HCl; (c) after 72 h of immersion in 1.02 g/L EE*Eh* + 0.5 M HCl.

Surface morphology of MS coupons was also studied by carrying out optical microscopy (OM) in aggressive medium without (blank) and with various concentrations of EE*Eh* at room temperature. Fig.9 (a to c) shown below are the optical micrographs of surface treated metal surface, without additive and with additive in aggressive medium. It is clear by the images that the addition of EE*Eh* in test solution diminishes the degradation of metal coupons.

Fig. 9: Optical micrographs of (a) surface treated MS coupon; (b) immersed in blank (without inhibitor) and (c) with additive (EE*Eh*) in 0.5 M HCl after 72 h immersion at 30°C.

H. Energy Dispersive X-Ray Analysis

The EDX analysis of MS surface was taken at few spots. The EDX spectrum in the absence of 0.5 M HCl Fig. 10 (a) shows the presence of large amount of FeO as indicated by the very high intensity of -O and Fe-signal. However, in the presence of 0.5 M HCl solution a high intensity of chloride ion peak is showing in Fig. 10 (b) and Fe containing -O peak which shows the contamination of aggressive media. The intensity of Fe and -O signal is significantly reduced in Fig. 10 (c) which is the spectrum of inhibited mild steel surface in 0.5 M HCl solution. The extract consist mainly of carbon (-C) and oxygen (-O) atoms, the variation of -C, chloride (-Cl) and -O weight percentage on the surface can be used quantitatively to explain the adsorption of extract.

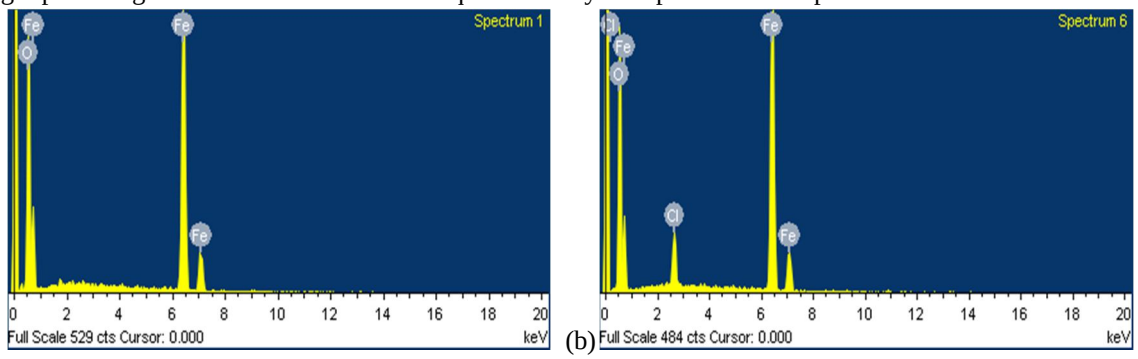

Due to the formation of Fe-inhibitor complexes formed on the metal surface in presence of EE*Eh*, the observed Fe-signal is reduced in Fig 10 (c) confirming the presence of inhibitor on to the metal surface. It is also found that the intensity of free oxygen is decreased due to the adsorption of carboxyl and hydroxyl group of many constituents of the inhibitor. Thus it can be concluded that the MS surface has a protective film of Fe^{2+}- EE*Eh* complex [38]..

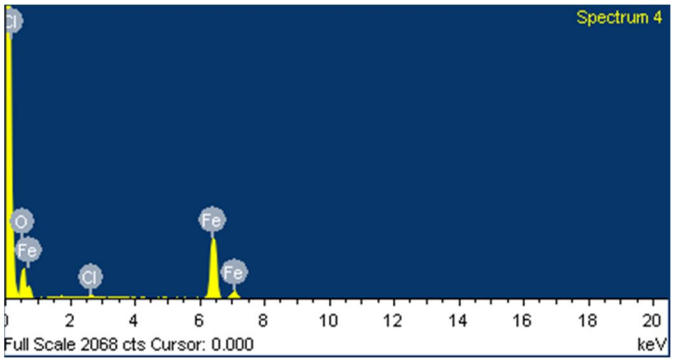

Fig.10: EDX-spectrum of (a) surface treated MS coupon; (b) MS immersed in without inhibitor (blank) in 0.5 M HCl (c) MS immersed in 0.5 M HCl with 1.02 g/L EE*Eh* additive.

IV. CONCLUSIONS

A. The inhibitory efficacy of Ethanolic extract of *Euphorbia hirta* (EE*Eh*) for Mild Steel in aggressive medium containing 0.5 M HCl without and with inhibitor was studied by chemical method, quantum chemical study and various surface morphological measurements, all the studies employed in the present study reveals the EE*Eh* has good adsorptive propensity for MS.

B. Inhibition efficiency was found to be maximum 84.07 % at 1.02g/L EE*Eh*. The corrosion inhibition is probably attributed to the phytochemical constituents present in the plant extract which block the active sites on metal surface by the phenomenon of physical adsorption.

C. The mechanism of adsorption is followed Langmuir adsorption isotherm. The negative values of free energy of adsorbtion reveal strong and spontaneous adsorption of inhibitor on to MS surface.

D. Quantum chemical study shows the reactive centre of various active constituents of inhibitor.

E. Spectroscopic studies viz. UV-Visible and FT-IR shows the formation of inhibitor EE*Eh*-Fe complex which is in good agreement with the good anticorrosive activity of EE*Eh*.

F. Surface morphological study by AFM, SEM, EDX and OM confirms that the MS coupon surface has smoothened due to the adsorption of phytochemicals over its surface, i.e., formation of a compact protective film of Fe^{2+}-EE*Eh* complex over the metal surface thereby impeding the dissolution of mild steel in aggressive medium at room temperature.

V. ACKNOWLEDGMENTS

The authors are greatly thankful to the Head, Department of Chemistry, University of Rajasthan, for providing necessary research facility and UGC for providing the financial support. Authors are also thankful to USIC, University of Rajasthan, Jaipur for supportive characterization techniques and tools.

REFERENCES

[1] Moore J. J., Corrosion of Metals. A text book of Chemical Metallurgy, Butterworth-Heinemann Ltd, Boston, New Jersey, 1994.
[2] Pierre, R. R., Corrosion Engineering: Principles and Practice, 1st ed., McGraw-Hill, New York, 2008.
[3] Fontana, Mars G., Corrosion Engineering, 2nd ed., Tata McGraw Hill, New Delhi, 2005.
[4] Zaferani, A.H., Sharifi M., Zaarei, D., Shishesaz M.R., J. Environm. Chemical Eng. 167, 6-15, 2013.
[5] Twite, R.L., Bierwagen, G.P., Prog. Org. Coatings., 33(2), 91-100, 1998.
[6] Sinko John, Prog. Org. Coatings., 42 (3), 267–282, 2001.
[7] Nair, R.N., Kharia, N., Sharma, I.K., Verma, P.S. and Sharma, J. Electrochem. Soc. India. 56 (1/2), 41-47, 2007.
[8] Nnanna, L.A., Anozie, I.U., Avoaja, A.G.I., Akoma, C.S., Eti, E.P., Afr. J. Pure Appl. Chem., 5(8), 265-271, 2011.
[9] Sharma, A., Nair, R.N., Sharma, A., Choudhury, G., Int. J. Adv. Scien. Tech. Res., 2(6), 713-729, 2012.
[10] Sharma, S., Parihar, P.S., Nair, R.N., Verma, P.S., Sharma, A., RASAYAN J. Chem. 5(1), 16-23, 2012.
[11] Sharma, A. and Sharma, S. K., Green Corrosion Inhibitors: Status in Developing Countries in Green Corrosion Chemistry and Engineering: Opportunities and Challenges, Wiley-VCH Verlag GmbH & Co. KGaA; pp. 157-180, 2012.
[12] Eduok, U.M., Umoren, S.A., Udoh, A.P., Arab. J. Chem. 5, 325–337, 2012.
[13] Sharma, A., Choudhary, G., Sharma, A., Yadav, S., Int. J. Innovative Res. Sci, Eng. Technol., 2, 7982-7992, 2013.
[14] Raja, P. B., Fadaeinasab, M., Qureshi, A. K., Rahim, A. A., Osman, H., Litaudon, M. and K. Awang, Ind. Eng. Chem. Res., 52, 10582−10593, 2013.
[15] Suedile, F., Robert, F., Roos, C., Lebrini, M., Electrochimica Acta 133, 631–638, 2014.
[16] Kumar, S., Malhotra, R., Kumar, D., Pharmacogn. Rev., 4, 58-61, 2010.
[17] Chitra, M., Muga,V., Dhanarasu, S., Al-hazimi A. M., J. Chem. Pharm. Res., 3(6), 110-114, 2011.
[18] Sharma, Alka, Sharma, Arpita, Choudhary, Guddi, Yadav, Swati, Int. J. Sci. Advanced Technol., 2(12) 68-74, 2012.
[19] Choudhary, Guddi, Sharma, Arpita, Sharma, Alka, Int. J. Innovative Res. Sci., Eng. Technol., 2(10) 5467-5478, 2013.
[20] Gokhan Gece, Corros. Sci., 50, 2981–2992, 2008.
[21] Gokhan, G., Semra, B., Corros. Sci., 52, 3304-3308, 2010.
[22] Wang, X., Wan, Y., Zeng, Y., Yaxin, G., Int. J. Electrochem. Sci., 7, 2403 – 2415, 2012.
[23] Obi-Egbedi, N.O., Obot I.B., Eseola A.O., Arab. J. Chem., 7, 197–207, 2014.
[24] Khaled, K.F., Abdel-Rehim, S.S., Saker, G.B., Arab. J. Chem. 5, 213-218, 2012.
[25] Oguzie, E. E., Chinonso, B. A., Conrad, Enenebeaku, K., Ogukwe, C.E., J. Phys. Chem. C., 116, 13603−13615, 2012.
[26] Hussin, M. H., Kassim, M. J., Int. J. Electrochem. Sci., 6, 1396–1414, 2011.
[27] Singh, A., Ebenso, E.E., Quraishi, M.A., Int. J. Electrochem. Sci., 7, 8543 – 8559, 2012.
[28] Leelavathi, S., Rajalakshmi, R., J. Mater. Environ. Sci., 4 (5), 625-638, 2013.
[29] Chebouat, E., Dadamouss, B., Gherraf, N., Gouamid, M., Allaou1i, M., Cheriti, A., Int. J. Electrochem. Sci., 8, 12147 – 12153, 2013.
[30] D. Senthil Vadivu, R. Saratha, R. Vasantha Jothi, Int. J. Sci. Eng. Technol. Res., 5 (12) (2016) 3324-3340.
[31] Xingwen Zheng, Min Gong, Qiang Li, Int. J. Electrochem. Sci., 12 (2017) 6232 – 6244.
[32] Siaka, O.E., Atiku, A.A, Muhmmad A.F.A., Innov. Sci. Eng., 1, 79-91, 2011.
[33] Harek, H., Touzani, R., Hammouti, B., Bouklah, M., Harek, Y., Arab. J. Chem., 5, 163–166, 2012.
[34] Udhayakala, P., Rajendiran, T.V., J. Chem., Bio. Phys. Sci., 2 (1), 172-183, 2012.
[35] S. A. Umoren, U. M. Eduok, M. M. Solomon, A. P. Udoh, Arabian J. Chem., 9 (1) (2016) S209-S224.
[36] Sangeetha, M., Rajendran, S., Sathiyabama, J., Prabhakar, Int. Res. J. Environment. Sci., 1(5), 14-21, 2012.
[37] Karthik, G., Sundaravadivelu M., ISRN Electrochemistry 1, 1-10, 2013.
[38] Amin, M.A., J. Appl. Electrochem., 36, 215, 2006.

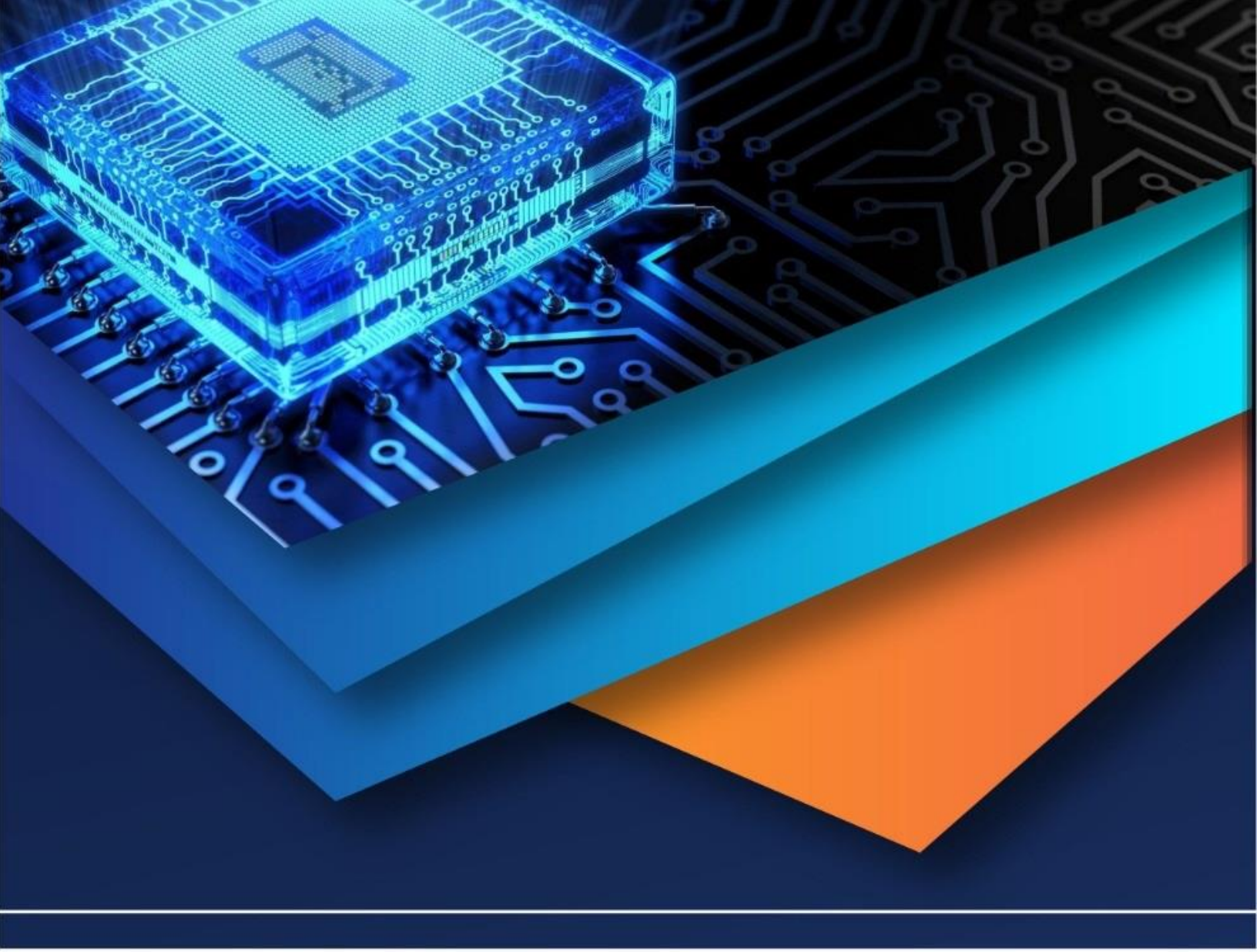

10.22214/IJRASET

45.98

IMPACT FACTOR: 7.129

IMPACT FACTOR: 7.429

INTERNATIONAL JOURNAL FOR RESEARCH

IN APPLIED SCIENCE & ENGINEERING TECHNOLOGY